C. R. Mecanique 345 (2017) 21–34

Contents lists available at ScienceDirect

Comptes Rendus Mecanique

www.sciencedirect.com

Basic and applied researches in microgravity/Recherches fondamentales et appliquées en microgravité

Nucleate pool boiling in microgravity: Recent progress and future prospects

Catherine Colin *, Olivier Kannengieser, Wladimir Bergez, Michel Lebon, Julien Sebilleau, Michaël Sagan, Sébastien Tanguy

Institut de mécanique des fluides de Toulouse, Université de Toulouse (INP–UPS–CNRS), 2, allée du Professeur-Camille-Soula, 31400 Toulouse, France

ARTICLE INFO

Article history:
Received 8 April 2016
Accepted 1 June 2016
Available online 9 November 2016

Keywords:
Pool boiling
Bubble dynamics
Heat transfer
Microgravity

ABSTRACT

Pool boiling on flat plates in microgravity has been studied for more than 50 years. The results of recent experiments performed in sounding rocket are presented and compared to previous results. At low heat flux, the vertical oscillatory motion of the primary bubble is responsible for the increase in the heat transfer coefficient in microgravity compared to ground experiments. The effect of a non-condensable gas on the stabilisation of the large primary bubble on the heater is pointed out. Experiments on isolated bubbles are also performed on ground and in parabolic flight. The effect of a shear flow on the bubble detachment is highlighted. A force balance model allows determining an expression of the capillary force and of the drag force acting on the bubble.

1. Introduction

Liquid vapour flows exist in a wide variety of applications in both normal gravity and reduced gravity environments. As it is usually the case, there are many benefits and drawbacks in the use of two-phase systems and, consequently, serious considerations are needed before deciding on whether or not to proceed with the design, construction and use of these systems, particularly in a reduced-gravity context.

In normal gravity, or terrestrial applications, gas–liquid flows have been traditionally studied by the petroleum and nuclear industries. The petroleum industry has focused most of their efforts on flow through long pipelines with the intent of transferring a mixture of crude oil and natural gas from the well and then performing the separation of the components or products at the refinery. The nuclear industry has been concerned with system stability and safety with the primary intent of preventing dry out of the nuclear reactor through either a heat transfer/fluid flow instability or loss of coolant accident as the heat energy is transferred from the reactor to the turbines. The chemical industries have utilised gas–liquid contactors to increase interfacial heat and mass transfers in absorption, stripping and distillation processes that involve two-phase flow though complex geometries.

In a reduced gravity environment, the principles remain the same. The applications concern the thermal management systems for satellites, the power managements systems for long time missions or manned space platforms, and fluid management from the storage tanks through the lines to the engine. Thermal management systems transfer heat from a source

* Corresponding author.
E-mail address: colin@imft.fr (C. Colin).

http://dx.doi.org/10.1016/j.crme.2016.10.004

(resistance heat from electronic equipment) to a sink, typically through a radiator panel. Different devices are used depending on the power to be transferred: heat pipes, loop heat pipe, single-phase mechanical pumped loop.

Another important problem concerns fluid management: the behaviour of the propellant in the tanks of the launchers and the transfer from the tank to the engines through the supply lines. The cryogenic liquids are pressurised by their vapour or a non-condensable gas. During the different phases of the mission (propelled phase, ballistic phase) it is important to control the phase distribution and the evolution of temperature and pressure inside the reservoirs. The evolution of these parameters strongly depends on heat and mass transfers. During the ballistic phase of the mission, the tank wall is heated by solar radiation and thermal dissipation due to engine and electrical devices. Since there is no thermal convection in microgravity, the heat transfer between the heated wall and the liquid is mainly due to heat conduction, and the wall temperature can become greater than the required temperature for the onset of nucleate boiling. The study of boiling in microgravity is thus of particular interest in this situation.

However, boiling is a complex phenomenon, which combines heat and mass transfers, hydrodynamics, and interfacial phenomena. Furthermore, gravity affects the fluid dynamics and may lead to unpredictable performances of thermal management systems. It is thus necessary to perform experiments directly in (near) weightless environments. Besides the ISS, microgravity conditions can be simulated by means of a drop tower, parabolic flights on board an aircraft or a sounding rocket. Several studies on pool boiling in microgravity were performed for the last 50 years. We will focus our analysis on nucleate boiling on flat plates and also on boiling on an isolated nucleation site. Since this review is far to be exhaustive, additional information can be found in other previous reviews by Straub [1], Ohta [2], Di Marco [3,4], Kim [5].

The studies performed by the authors of this paper have been mainly supported by the French Space Agency CNES ("Centre national d'études spatiales") in the network GDR "Fundamental and Applied Microgravity" and in the COMPERE Programme (Behaviour of propellants in tanks) or Programme of the European Space Agency (MAP Project: Multiscale ANalysis of BOiling). The first part of this paper is devoted to the studies of pool boiling in microgravity on heated plated. The second part concerns the behaviour of isolated bubbles with the characterisation of local wall heat transfer and the study of bubble hydrodynamics.

2. Pool boiling on flat plates in microgravity

2.1. Boiling regimes

The study of pool boiling in microgravity has begun in the 1960s with the NASA Space programme with experiments performed during short test time in drop towers by Merte and Clark [6] or Siegel [7]. During the 1980s and the 1990s, experiments on flat heated plates have been carried out during longer microgravity periods in parabolic flights, sounding rockets or aboard the space shuttle by Zell et al. [8], Lee et al. [9], Ohta [10] and Oka et al. [11], Straub [1]. These experiments have shown the existence of stable boiling regimes in microgravity over long periods. In a review of these experiments, Straub [1] remarked that gravity has a relatively weak influence on heat transfer in nucleate boiling, but it strongly affects the dry out of the heated plate, reducing significantly the critical heat flux in microgravity. These experiments were performed with different fluids, mainly refrigerants R11, R12, R113, R123, on flat plates of different sizes, at different reduced pressures, liquid subcoolings.

First, the onset of nucleate boiling appears for a lower wall superheat in microgravity compared to 1-g with an upward facing plate. In normal gravity, thermal convection cools down the heated plate and delays the onset of nucleate boiling. Then different nucleate boiling regimes are observed. In the experiments of Lee et al. [9], Ohta [10] and Oka et al. [11], one large bubble is levitating over the heated surface. It is separated from the wall by a liquid layer in which many very small bubbles are nucleated, grow and coalesce with the large bubble, which oscillates up and down due to coalescence events, but never touches the wall.

In other experiments [8], the large bubble is in contact with the wall and covers a significant part of the heated surface. Its size is controlled by heater size, wall superheat, and liquid subcooling. Other small bubbles are nucleated around the larger one and coalesce with it. This boiling regime is rather observed on small heated plates or at high heat flux. If liquid subcooling is sufficiently high, the bubble may keep a constant size on the wall, balanced by evaporation at its foot and condensation at its top. If subcooling is too low, the large bubble expands over the heated surface and a dry-out of the surface occurs. A large bubble is observed when the microgravity level is very low, in sounding rockets or space shuttle experiments. In parabolic flight, due to g-jitter, smaller bubbles are observed near the heated surface. They are detached or swept by g-jitter. A large bubble is not observed for low heat fluxes when liquid subcooling is high. Bubbles nucleate on the wall, quickly coalesce after their detachment, and sometimes even before.

The influence of pressure was studied by Straub [1], who clearly showed that in earth gravity conditions, an increase of pressure causes an increase of heat transfer. The effect of liquid subcooling on heat transfer has been studied by several authors like Lee et al. [9], Ohta [10] or Oka et al. [11]. Unfortunately, in most of these experiments, subcooling was changed by varying the pressure. It is therefore difficult to distinguish separately the effect of subcooling and pressure on the change in heat transfer. Recent experiments of Kannengieser et al. [12] with a controlled pressure showed that subcooling had no influence in the fully developed boiling regime, when the bubbles cover the whole heated plate. For low heat fluxes, heat transfer is enhanced in microgravity compared to the case of a 1-g upward facing plate and decreased compared to the case of a 1-g downward facing plate.

The effect of an electric field on bubble dynamics and heat transfer was also studied. Di Marco and Grassi [13] conducted pool-boiling experiments with FC72 on a 2 cm ×2 cm heated surface aboard the Foton M2 satellite at a pressure of 1 bar. Without electric field, they found that heat transfer is lower in microgravity compared to 1-*g* conditions. As the electric field is applied in microgravity, the bubbles detach from the wall, then the void fraction decreases, coalescence diminishes and heat transfer is improved. For the highest electric field close to 10 kV, similar heat transfer is observed in microgravity and in 1-*g*, and the boiling crisis is delayed. More recently, experiments were performed on a small micro heater array in parabolic flights [14].

Since the 2000s, several experiments were performed with local measurements of the heat flux or wall temperature for a better understanding of the physics of boiling. Ohta [10] performed pool boiling experiment on a transparent heater in parabolic flights. It allows both the observation of the macro layer or micro layer behaviour from underneath and the measurements of local surface temperatures and of the layer thickness. Tiny bubbles were observed in the macro layer underneath the large bubble formed at high heat flux. Evaporation at the foot of the primary bubbles dominates heat transfer in microgravity. No dry patch was observed in these experiments.

Experiments on pool boiling of FC72 and *n*-perfluorohexane at 1 bar were performed at a surface with controlled wall temperature thanks to micro heater arrays in parabolic flights by Kim et al. [15], Christopher and Kim [16], Raj and Kim [17], Raj et al. [18–20] and more recently aboard the International Space Station [21]. The heater size was varying from 2 mm × 2 mm to 7 mm × 7 mm and contained up to 10 × 10 micro heaters kept at constant temperature. This measurement technique allowed measuring the distribution of wall heat flux below the bubbles growing on the wall. Since the heater was transparent, video recordings taken from below the heater allowed us to visualise the contact lines at the bubble foots. The micro heaters had a very short response time, thus it was possible to investigate the variation of heat flux during the transient phase from 1.8-*g* to 0-*g* and 0-*g* to 1.8-*g* in parabolic flights. The effects of residual gravity, heater size, liquid subcooling, concentration of non-condensable gas were carefully checked, and scaling laws for the influence of these parameters on the heat transfer coefficient are provided [17,20,22].

Zhao et al. [23] studied pool boiling of FC72 on an alloy surface of 15 mm × 15 mm with a roughness of a few micrometres aboard the Chinese satellite SJ-8. The duration of the microgravity period was about 100 s, and quasi steady boiling was observed for subcooled regimes. In microgravity, small bubbles coalesce on the heater, leading to a large bubble, and the wall heat transfer was found to be smaller than on earth gravity for wall heat fluxes larger than 6 W/cm^2. The critical heat flux was also lower in microgravity than on earth. The amount of dissolved gas was not quantified in this experiment.

Recent experiments on pool boiling on a flat plate were also conducted in the Boiling eXperimental Facility (BFX) aboard the International Space Station by Warrier et al. [24] on an aluminium wafer with five artificial nucleation cavities. Several local heaters and thermistors were located on the backside of the wafer. Experiments were performed with isolated or multiple bubbles with perfluoro-*n*-hexane at different pressures and with a dissolved gas concentration around 260 ppm. After boiling incipience, the bubbles stayed on the wall and coalesced to a large bubble in the centre of the heater. As the heat flux increased, new bubbles were nucleated and coalesced with the large bubble. The large bubble might cover the wall heater surface and sometimes lifted-off but levitated just above the heater and small bubbles nucleated on the wall continued to merge with the large bubble. The behaviour of the bubbles was similar to what had been previously observed by Lee et al. [9] and Straub [1]. The heat flux measured in natural convection and partial nucleate boiling is much smaller in microgravity than in normal gravity.

Most of these experiments were performed on very smooth surfaces. Kannengieser et al. [25,12] and Sagan [26] performed experiments on pool boiling on a heated copper plate of 1 cm^2, with HFE7000 as the working fluid in parabolic flights and also in two sounding rockets Maser 11 and Maser 12 for low-heat fluxes. In the sounding rockets, the test cell was a small cylindrical tank 60 mm in diameter and 217 mm in length, with spherical parts at both ends. The lateral surface of the tank was made of quartz for flow visualisations. The tank was connected at its lower part with a reservoir of liquid HFE7000. At its top, it was connected to a gaseous nitrogen tank in Maser 11 or to a pressurised vapour HFE7000 tank in Maser 12. A heated plate for the study of nucleate boiling was located at the bottom of the reservoir (Fig. 1). It consists of an electrical resistance heated by Joule effect in contact with a fluxmeter and a rough copper plate with a thickness of 40 µm (Fig. 2). The fluxmeter was equipped with two thermocouples. It was then possible to measure at the same time the heat flux transmitted to the liquid and the wall temperature. Five microthermocouples 100 µm in diameter were placed above the heated plate to measure the liquid or vapour temperature. Before the launch of the rocket, the tank was vacuumed and the metallic part at the top of the test cell was heated. Then the lateral quartz cylinder was also heated by conduction from the metallic part. After the rocket take-off when the microgravity phase was reached, the tank was partly filled with liquid HFE7000 and pressurised either by nitrogen or by its own vapour (Fig. 1). The free surface took a spherical shape. The liquid was subcooled and evaporated in contact with the heated quartz wall. The evaporation rate was high near the contact line. A strong mass transfer occurred at the interface between the subcooled liquid and the overheated vapour in Maser 12 (Fig. 1, right). In Maser 11, due to presence of a non-condensable gas, a strong Marangoni convection took place at the free surface. It stabilised the free surface and led to entrainment and dissolution of nitrogen into the liquid bulk. The concentration of nitrogen in the liquid was estimated to be close to 0.01 mol N_2/mol HFE7000 [25].

Different bubble behaviours were observed in the experiments on the ground, in parabolic flights, in sounding rocket without and with non-condensable gas (Fig. 3). In parabolic flights, the bubble size was smaller than in sounding rocket experiments. Due to *g*-jitter, the small bubbles lifted-off or slided on the heated wall, before having time to coalesce and form one large bubble. In the sounding rocket Maser 12, experiments were performed with pure liquid/vapour. The

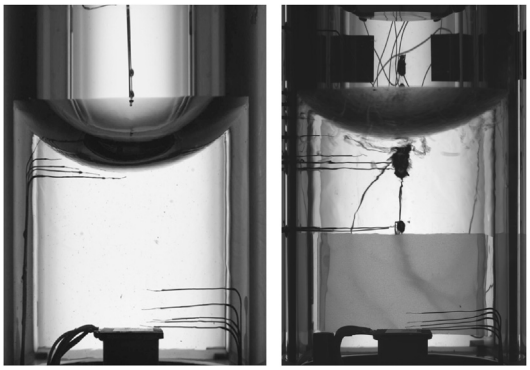

Fig. 1. Test cell: liquid HFE7000 pressurised by nitrogen in Maser11 (left) and vapour HFE7000 (right) in Maser12.

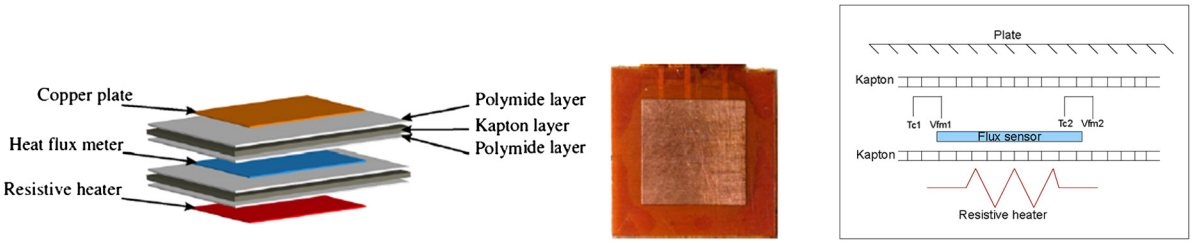

Fig. 2. Heater.

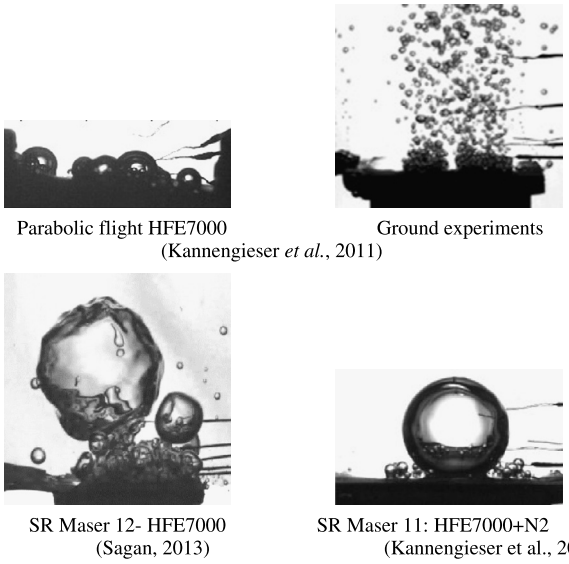

Fig. 3. Flow boiling regimes with HFE7000 (pure liquid–vapour system or with gaseous nitrogen) on a 1-cm^2 heated plate in microgravity: $q = 3$ W/cm^2, $P = 1$ to 1.5 bar, $\Delta T_{sub} = 5$ to 10 K.

runs consisted of three measurements at 1.5 bar with a liquid subcooling ΔT_{sub} of 10 °C and three wall heat fluxes q of 1.88 W/cm^2, 2.92 W/cm^2, and 3.6 W/cm^2. One experiment was also conducted at 1.3 bar at saturation with a heat wall flux of 1.7 W/cm^2. After boiling incipience, several vapour bubbles nucleated on the wall. It took about 20 s for the bubbles to coalesce and form one large bubble, which remained in the wall vicinity during all the flight. The bubble was sometimes attached to the wall, sometime detached from the wall. Different behaviours were observed in subcooled boiling and in saturated boiling. The wall temperature was measured by two thermocouples in the fluxmeter and the liquid temperature was measured by an array of thermocouples above the heater (Fig. 1). Thermocouples TC_{24} and TC_{23} are located 0.48 mm and 0.78 mm from the heated wall, respectively. For subcooled boiling, the values of $TC_{24} - T_{sat}$ and $TC_{23} - T_{sat}$, T_{sat} being the saturation temperature, are displayed in Fig. 4. The large bubble radius and the distance of the bubble foot to the wall are determined by image processing and also plotted in Fig. 4. The large bubble had a strong oscillating motion in the

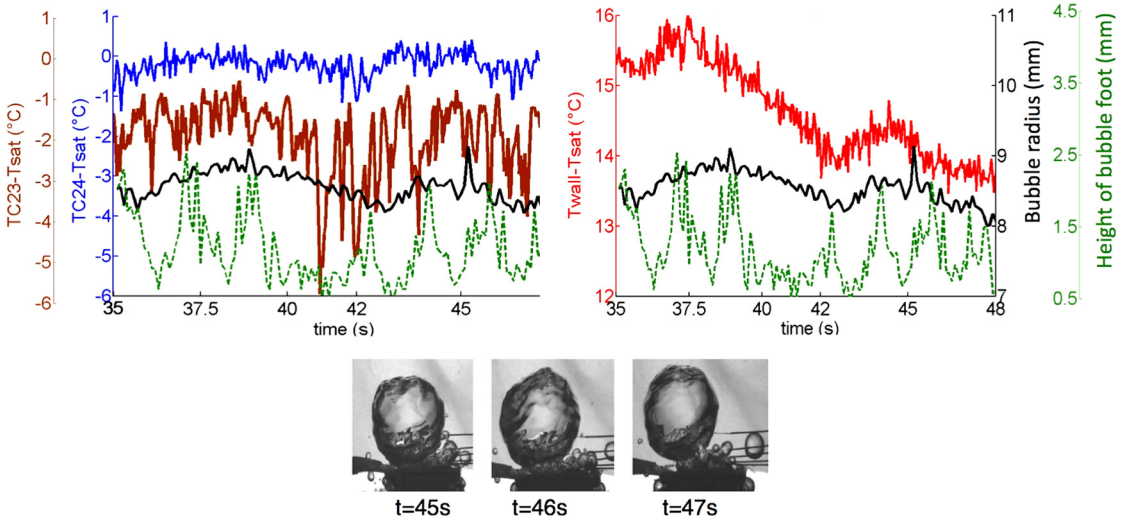

Fig. 4. Wall temperature and bubble size and height evolutions for $q = 2.92$ W/cm^2, $P = 1.5$ bar, $\Delta T_{sub} = 10\,^{\circ}$C [26].

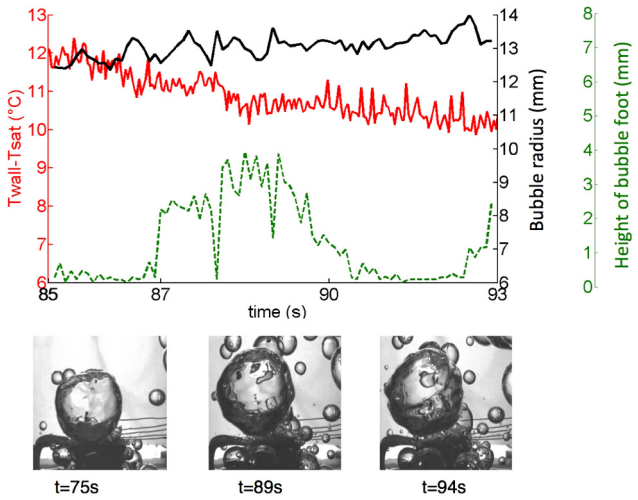

Fig. 5. Wall temperature and bubble size and height evolutions for $q = 2.92$ W/cm^2, $P = 1.3$ bar, $\Delta T_{sub} = 0\,^{\circ}$C [26].

vertical direction. The bubble size was controlled by the vaporisation on the wall and/or coalescence with small bubbles nucleated on the wall and the condensation at the bubble top. The thermocouples TC_{24} and TC_{23} can be either in the liquid phase or in the vapour phase since many bubbles nucleated on the wall. TC_{24} measured a liquid temperature close to T_{sat}, which was characteristic of the vapour or liquid temperature at saturation. The overheated liquid layer was smaller than 0.5 mm. The measurements of TC_{23} varies from the vapour temperature close to T_{sat} to the liquid temperature locally subcooled from 2 to 5 °C. The evolution of the bubble radius seems to be linked to the evolution of the liquid temperature in the wall vicinity. As the subcooling decreases, the bubble radius increases. The evolution of the bubble vertical motion is not directly correlated with the variation of its radius.

In saturated boiling conditions (Fig. 5), the bubble also had a vertical motion, but with a lower frequency than in subcooled boiling. It stayed longer periods on the wall ($85 < t < 87$ s and $90 < t < 92.5$ s) and levitated above the other bubbles also for a long period ($87 < t < 90$ s). The mean bubble radius increases from 12.5 to 13.5 mm. As the bubble levitated, liquid rewetted the wall and new bubble nucleation took place, leading to an increase in the heat transfer, which can be seen through the decrease in the wall temperature.

The vertical motion of the large bubble was not observed in the Maser 11 experiment with the presence of non-condensable gas. The large bubble remained stable on the heated plate. Small bubbles nucleated on the wall were driven by the Marangoni convection toward the large bubble and coalesced with it [25]. The different bubble behaviours observed in the experiments are responsible for the different evolutions of the boiling curves observed in normal and microgravity conditions.

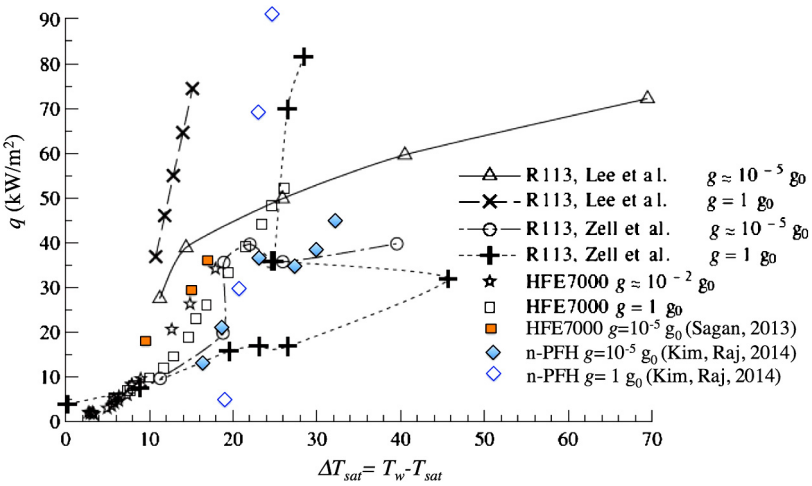

Fig. 6. Boiling curves in earth gravity and microgravity from Zell et al. [8] and Lee et al. [9] with R113, from Kim and Raj [27] with *n*-perfluorohexane and from Kannengieser et al. [12] and Sagan [26] with HFE7000, at a pressure of about 1 bar to 1.5 bar and a subcooling value of about 10 K.

2.2. Influence of gravity on heat transfer in nucleate boiling

Several correlations exist to predict heat transfer in nucleate pool boiling in earth gravity. These correlations often depend on gravity since the capillary length is taken as a characteristic length scale for the bubble size at detachment. Critical reviews of the application of these correlations to microgravity conditions were performed by Di Marco and Grassi [28], Straub [1] and Kannengieser et al. [12]. From these correlations, we can write the dependency of the wall heat flux on gravity as:

$$\frac{q}{q_0} \sim \left(\frac{a}{g_0}\right)^n \tag{1}$$

where q_0 is a reference heat flux taken at gravity g_0, generally terrestrial gravity. n is a constant, which varies from 0.3 to 1.5 for most of the usual correlations [29,30]. Except for the correlation of Cooper [31], where $n = 0$, the usual correlations anticipate a very low heat flux in microgravity, which is not in agreement with the experimental results. So, these correlations are not adequate to estimate the heat flux in microgravity and it is more relevant to use g as a constant equal to its value on earth, as suggested by Dhir [32]. In fully developed nucleate boiling regime in microgravity, the measurements of liquid temperature profile in the wall vicinity by Kannengieser et al. [12] shows that the thermal boundary layer is of the order of tens of micrometres, which is much smaller that the capillary length. This length scale is therefore more relevant than the capillary length to predict the wall heat transfer in microgravity conditions.

From the previous works it appears that the influence of different parameters like gravity or subcooling or heater size remains unclear. For example, Fig. 6 shows the comparison of two boiling curves on earth and in microgravity conditions obtained by Lee et al. [9] and Zell et al. [8] both for R113 on a flat plate with a gold coated heater. These experiments do not display the same trends: Lee et al. [9] pointed out an improvement of heat transfer in microgravity, whereas Zell et al. observed the opposite trend. For this last experiment, it was reported that the foot of the large bubble was increasing in size during the experiment and that a stable wall temperature has never been reached. At a heat flux of about 40 kW/m^2, the boiling curve in microgravity of Zell et al. [8] takes a low slope and, at the same value of heat flux, the boiling curve of Lee et al. [9] takes also a low slope and crosses the boiling curve in earth gravity condition. At this value of the heat flux, the two authors have reached the 'dry-out' heat flux. In the experiment of Zell et al. [8], the boiling curve in microgravity condition was under the boiling curve in earth gravity condition because most of the measurements have been performed above the 'dry out' heat flux. For this last experiment, nucleate boiling in earth gravity condition is compared to boiling in microgravity in a regime equivalent to film boiling.

Some data recently obtained by Kim and Raj [22] for the boiling of *n*-perfluorohexane on micro water heater arrays onboard the International Space Station are also plotted in Fig. 6. For this dataset, the size of the heater was 7 mm × 7 mm, and the subcooling was about 10 K. At a very low heat flux, heat transfer was larger in microgravity than in normal gravity. For wall superheat larger of 24 K, the bubble size reached the heater size in microgravity and the wall heat flux was limited to 45 kW/m^2, whereas it continued to increase in normal gravity up to 130 kW/m^2.

In Fig. 6 the experimental results obtained by Kannengieser et al. [12] in parabolic flights and Sagan [26] in the Maser 12 sounding rocket with HFE7000 are also plotted. In these experiments, the wall heat fluxes were lower than 40 kW/m^2. Heat transfer was larger in microgravity conditions than on earth and no dry-out was observed in these experiments. The heat flux was too low to observe the dry out and a deterioration of the heat transfer in microgravity compared to earth

gravity. The wall heat flux was a little bit larger in the sounding rocket experiment that in parabolic flights. This is probably due to the oscillating motion of the large bubble above the heater, enhancing heat transfer.

Several authors tried to predict the wall heat transfer in pool boiling in microgravity. Raj et al. [18–20,22] performed systematic experiments on microheater arrays to point out the effect of gravity, heater size, liquid subcooling and non-condensable gas concentration. They identified two heat transfer modes versus the gravity level. For the highest values of a/g (g being the terrestrial gravity), the Buoyancy Dominated Boiling regime (BDB) was observed. Bubbles grew and detached from the wall by the buoyancy force. For the lowest values of a/g, boiling regime was controlled by surface tension effects (Surface tension Dominated Boiling regime (SDB)). A large bubble appeared on the heater and smaller bubbles nucleated on the heater and coalesced with the large one. The transition between these two regimes depends on the heater width L_h compared to the capillary length L_c. If $L_h > 2.1L_c$, BDB regime was observed. For the BDB regime the value of the wall heat flux at any gravity level, is correlated to a reference value of the heat flux q_{ref} for an acceleration of a_{ref}:

$$\frac{q_{BDB}}{q_{ref}} = \left(\frac{a}{a_{ref}}\right)^{n_{BDB}} \quad n_{BDB} = \frac{0.65T^*}{1+1.6T^*} \quad T^* = \frac{T_w - T_{ONB}}{T_{CHF} - T_{ONB}} \tag{2}$$

The exponent n_{BDB} is expressed versus the dimensionless wall temperature T^*, which is function of the temperature at the onset of nucleate boiling, T_{ONB}, and of the temperature measured for the critical heat flux T_{CHF}. This expression was established for various heater sizes, liquid subcoolings, wall heat fluxes, and non-condensable gas concentrations. In the SDB regime, the dependency on the gravity level is lower, with $n_{SDB} = 0.025$ from parabolic flight experiments and $n = 0$ for ISS experiments. At the transition between BDB and SDB regimes, a jump in the wall heat flux is observed. This jump is linked to the concentration of non-condensable gas and is function of a Marangoni number Ma. Then the heat flux in the SDB regime is expressed as follows:

$$q_{SDB} = q_{BDB}\left(\frac{a_{trans}}{a_{BDB}}\right)^{n_{BDB}}\left(1 - e^{C_{Ma}}\right) \tag{3}$$

where a_{trans} is the acceleration for which $L_h = 2.1L_c$ and $C = 8.3 \cdot 10^{-6}$ for FC72. Equations (2) and (3) are able to predict the wall heat flux in BDB and SDB regimes for a wide range of heater sizes, liquid subcoolings, non-condensable gas concentrations. The interest of this correlation is that it uses a reference value of the wall heat flux at a reference gravity level. This value of q_{ref} is a function of the wall properties and especially of the nucleation site density, which is a parameter difficult to quantify and control. Then the use of Equations (2) and (3) takes into account de facto the surface properties.

Nevertheless, these correlations always predict a lower value of the wall heat flux in microgravity than on earth gravity, which is not always the trend experimentally observed, especially at low heat flux for larger heated plates. In the experiments performed by Kannengieser et al. [12] in microgravity, the nucleate boiling regime was fully developed. Bubbles covered the whole heated surface and the temperature profiles measured in the liquid showed that the overheated layer close to the wall had a thickness of tens of micrometres, indicating that heat transfer was controlled by mechanisms occurring in the near-wall region, as bubble nucleation, coalescence, motion of contact lines. Then Kannengieser [33] determined the more relevant dimensionless numbers to characterise heat transfer. The relevant physical properties and parameters are liquid and vapour densities ρ_L and ρ_V, liquid viscosity μ_L, thermal conductivity λ_L, heat capacity C_{PL}, surface tension σ, latent heat of vaporisation h_{LV}, wall heat flux q, wall superheat $\Delta T_{sat} = T_w - T_{sat}$, acceleration a, expansion coefficient β; the thermal conductivity, the heat capacity of the vapour are supposed to have negligible influence. Considering that the heat flux can be expressed versus 11 parameters, expressed versus four dimensions (length, mass, time, energy), seven independent dimensionless numbers can be built:

$$Ja = \frac{C_{PL}(T_w - T_{sat})}{h_{LV}} \quad Pr = \frac{\mu_L C_{PL}}{\lambda_L} \quad R = \frac{\rho_L}{\rho_V} \quad Ca = \frac{\mu_L V}{\sigma} \quad Fr = \frac{V^2}{aL}$$
$$Ri = \frac{V^2}{aL\beta(T_w - T_{sat})} \quad Ec = \frac{V^2}{C_{PL}(T_w - T_{sat})} \tag{4}$$

The Eckhert number Ec is very small in all the experiments. In microgravity, the inverse of the Richarson and Froude numbers $1/Fr$ and $1/Ri$ are very small, then only four dimensionless numbers will be considered to predict heat transfer in microgravity: the Jacob number Ja, the Prandtl number Pr, the density ratio R and the capillary number Ca. A relevant velocity scale V for the liquid motion in the overheated layer is due to vaporisation: $V = q/(\rho_V h_{LV})$. The following correlation was derived to predict the wall heat flux at different pressures for HFE7000 in microgravity conditions (Fig. 7):

$$Ca = \frac{\mu_L q}{\sigma \rho_V h_{LV}} = 4.5 \cdot 10^{-3} R^{0.85} Pr^{-1.5} Ja^{1.8} \tag{5}$$

This work was performed in the frame of the COMPERE programme of CNES to predict heat and mass transfer in the launcher tanks. Experiments of boiling liquid oxygen in magnetic compensation were also performed by Air Liquide at CEA Grenoble [33]. Despite the wall heat flux was five times larger with liquid oxygen than with HFE7000, Eq. (5) is also able to predict the heat transfer of boiling liquid oxygen at different pressures (Fig. 8). It can be explained by the fact that in the liquid oxygen experiment, the nucleate boiling regime was also fully developed. In order to include the effect of gravity on

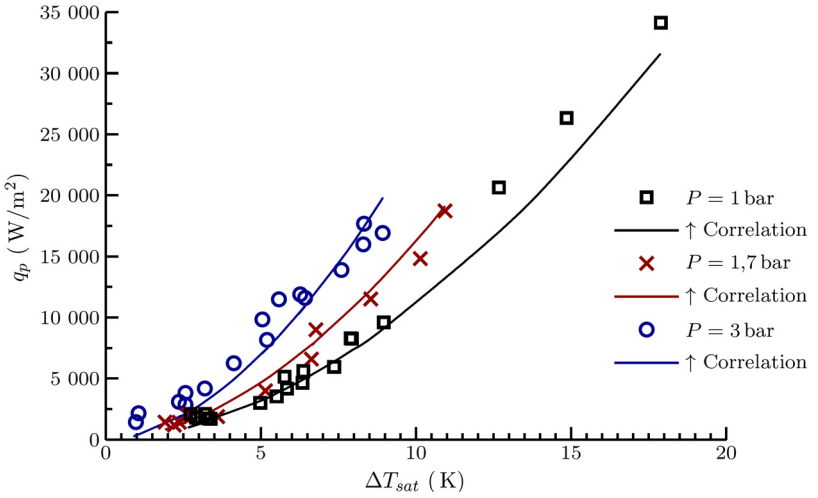

Fig. 7. Wall heat flux in microgravity for HFE7000, comparison with correlation (5).

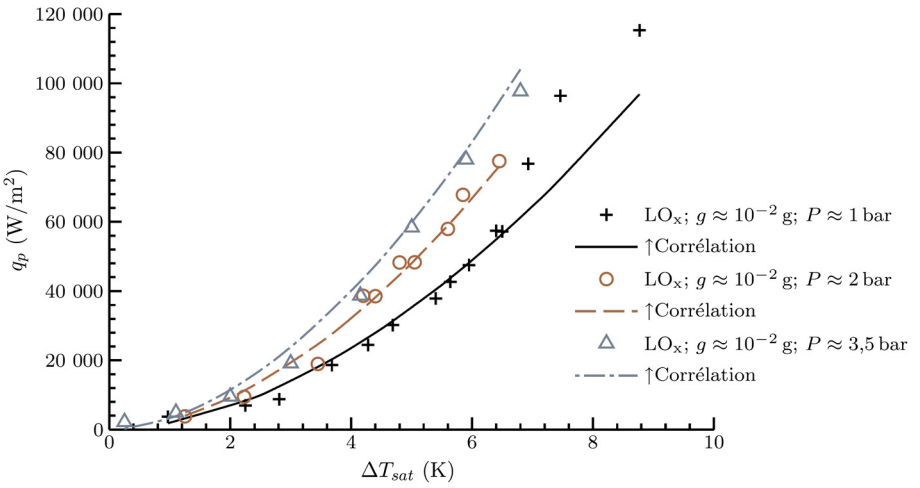

Fig. 8. Wall heat flux for liquid oxygen in microgravity (magnetic compensation), comparison with correlation (5).

heat transfer, the *Ri* and *Fr* numbers should be taken into account. It is important to notice that the length scale involved in these numbers is a length scale characteristic of the overheated layer near the wall (a conduction length) and not the capillary length usually taken into account in the correlations [33].

Despite the number of experiments on pool boiling in microgravity performed over the past 50 years, the prediction of boiling heat transfer remains a difficult task. Correlations are very useful, especially for industrial applications, even if they have a limited range of validity. The difficulty to predict heat transfer in nucleate boiling both in normal and microgravity conditions can be easily understood, regarding the numerous involved mechanisms: bubble nucleation, evaporation at the contact line, re-condensation, coalescence, bubble detachment, sliding on the wall...

3. Boiling on isolated nucleation site

In the 2000s, thanks to the improvement of measurement techniques and numerical methods, several studies were performed at the bubble scale for a better understanding of the mass, momentum and heat transfers involved in nucleate boiling. Bubble detachment under an electric field or in a shear flow was also investigated. In this session, we will summarise some previous and recent results and give some prospects.

3.1. Heat and mass transfers around a single bubble

Several experiments have been focused on boiling on an isolated nucleation site by Qui and Dhir [34], Qui et al. [35] and Sodtke et al. [36], Schweizer and Stephan [37]. The heat and mass transfer around a single bubble was investigated using high-resolution measurement techniques to characterise the local heat flux at the wall and in the thermal boundary layer.

Several experiments were performed in parabolic flight to visualise the periodically moving local temperature minimum at the wall underneath the 3-phase contact line, either using thermochromic liquid crystals [36,38] or high-speed infrared thermometry [39,37]. Some experiments were also carried out in free-floating during the parabolic flights to reduce the effect of g-jitter. Thanks to these local measurements and those performed by Kim et al. [15], Christopher and Kim [16], Ohta [10] the different mode of heat transfer from the wall to bubble and the liquid bulk were highlighted. The strong decrease in the wall temperature close to the three-phase contact line is due to a strong evaporation in this region. Several authors [40–42] developed theoretical analyses of the evaporation near a moving contact line to predict the local heat flux and the evolution of the apparent contact angle. The experiments in microgravity provide good validation tests for these theoretical models, because the bubble size and growth time are much larger than on earth. It is therefore easier to obtain time and space resolved measurements of temperature and heat flux at the bubble foot.

Direct Numerical Simulation were developed in parallel to these experiments. Balance equations for mass, momentum and energy are solved in the two-fluid domains using the 'volume of fluid' or 'level set' methods. The resolution of these equations is coupled with microlayer evaporation models near the contact line [43,35,44–46,26]. The results of these numerical simulations are in good qualitative agreement with the experimental results.

3.2. Effect of an electric field on bubble detachment

Electric fields have been shown to mitigate the effects of reduced gravity on boiling heat transfer by providing a body force on the bubbles. These forces may be conceived to press bubbles against the surface, increasing heat transfer, or to remove them away, delaying boiling crisis. In recent experiments in parabolic flights [14], boiling of FC72 was generated on a microheater array of 7 mm $\times$ 7 mm. An external electric field up to 10 kV was imposed over the boiling surface by means of a grid of four rods parallel to the heater. The effect of electric field led to a reduction in the bubble detachment diameter and an increase in the heat transfer compared to microgravity without electric field. This effect is less important as the heat flux increases.

Di Marco [47] writes a balance of the forces acting on an isolated bubble under an electric field. During a quasi-static bubble growth, these forces are the buoyancy, internal overpressure, surface tension at the bubble foot and electric forces. The evaluation of the electric force is not trivial due to the fact that the electric field configuration is continuously modified by bubble growth. Cattide et al. [48] used experimental bubble shapes to compute the electric field and the Maxwell stress tensor, with the aid of the code COMSOL Multiphysics. They assumed a non-conductive fluid with no charge at the interface. The resulting force tends to elongate the bubble. Experimental results were also compared with direct numerical simulations [49]. This phenomenon is even more complex in boiling and work has still to be done for a better understanding of the effect of an electric field on the detachment of a vapour bubble.

Even if these experimental activities have widely clarified the role of electric forces in boiling and in bubble growth in microgravity [50], further investigation is needed to understand the role played by the fluid properties, the action of electric forces at the bubble foot, in the region around the three-phase line, and to optimise the electric field configuration in order to reduce the applied voltage to the minimum possible.

3.3. Bubble detachment in a shear flow

The growth and detachment of vapour bubbles in a shear flow on a heated surface is one of the basic mechanisms that have to be understood to improve the modelling of heat transfer in convective nucleate boiling. Bubble vaporisation at the heated wall of a liquid flow has been experimentally investigated *under normal gravity conditions*. Thorncroft et al. [51] published a review of experimental results on bubble detachment in pool and convective boiling on horizontal and vertical surfaces. They showed that at low liquid flow rate, on horizontal surfaces, buoyancy detaches the bubble perpendicularly to the wall. As the liquid flow rate is high, the bubble does not lift off, but slides on the heated wall under the effect of the liquid drag force. On the vertical wall, the bubble slides on the wall for a long time before lifting-off. Point force models are often used to predict the bubble detachment diameter [52]. The main difficulty is to model the forces acting on the bubble during its growth. Drag and lift coefficients are unfortunately unknown for a bubble growing on the wall at intermediate bubble Reynolds numbers (10 to 200). Some experiments on ground [53] and direct numerical simulations for hemispherical bubbles [54] provided some expressions of the drag and lift forces. The evaluation of the capillary force requires the values of the contact angles at the bubble foot and the width of the bubble foot in contact with the heated plate.

In microgravity, bubble vaporisation on heated surfaces has been mainly studied in pool boiling. Ma and Chung [55] however reported experiments in which a single vapour bubble was nucleated and grown in flow field of FC-72 on a flat surface in terrestrial gravity and microgravity. They showed that the increase in the liquid flow rate slows down the growth of the bubble. Forced convection also enhances the departure of bubbles from their nucleation sites. In microgravity, the bubble diameter is larger than at 1-g. The influence of buoyancy disappears, as the liquid flow rate is high. Another study was performed in 2D configuration in a Hele–Shaw cell (Serret et al. [56]). The bubble was created on a heated flow and two cameras were used on both sides of the channel: one visible camera to record the bubble shape and one infrared camera to measure the temperature field in the liquid surrounding the bubble.

Another set of experiments was performed a in rectangular channel of cross section 40 mm in width, 5.69 mm in height and 650 mm in length [57–59]. A refrigerant HFE7000 was circulated in the channel with velocities up to 0.3 m/s

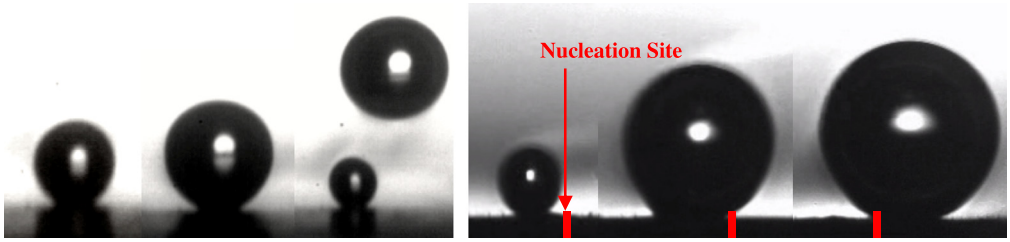

Fig. 9. Growth and detachment of a vapour bubble in a shear flow on ground 1-g (left) and in a micro-gravity conditions μ-g (right). The liquid flow velocity of 0.113 m/s is from left to right.

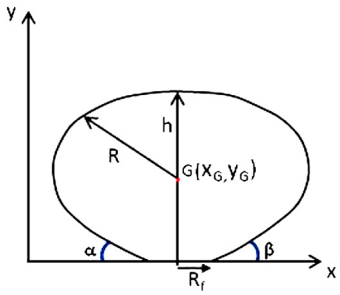

Fig. 10. Geometrical parameters deduced from image processing.

corresponding to a flow Reynolds number of 9000. For the experiments, liquid subcooling was about 10 K. Isolated bubbles were nucleated on a bubble generator, which is a thin layer (∼200 nm) of gold sputtered on a glass substrate. A cavity of mouth size around 50 µm on the layer provided a nucleation site and made possible the single vapour bubble generation.

Experiments were performed on ground with the horizontal channel and in microgravity during parabolic flight experiments. The dynamic of the bubble growth and detachment was recorded with a high-speed video camera PCO 1200 HS at frequencies of 500 images per second with 1200 × 1024 pixels (the field of view was 2.4 mm × 2 mm and the resolution was 508 pixels/mm). All the acquisitions were performed by shadowgraphy. By means of a light source, a parallel beam illuminates the bubble so that it appears in black on a white background (Fig. 9). From image processing using Matlab software, the bubble contour was identified and the geometrical parameters (Fig. 10) can be evaluated: equivalent radius R, apparent foot radius R_f, contact angles α and β, coordinates of the centre of gravity in the horizontal and vertical directions x_G and y_G, bubble volume V_b.

The nucleated bubble grew with time until its departure from the nucleation site as shown in Fig. 11 for both normal and microgravity conditions. A fitting curve of the bubble radius R during the growth has a time dependency $R \sim t^{1/3}$, which is slower than the diffusion control growth proportional to $t^{1/2}$. This might be a result of the re-condensation of vapour at the bubble top, where a luminous plume indicating heat transfer was typically observed in liquid flow (Fig. 9). In 1-g, the bubbles lifted off, whereas the bubbles slided parallel to the wall in μ-g. After its departure, the bubble decreased in size through re-condensation in the subcooled liquid. The bubble radius at detachment varied between 0.12 and 0.2 mm on the ground and between 0.18 and 0.25 mm in μ-g. In Fig. 11, the bubble foot radius R_f is also plotted. In normal gravity, the time of lift-off ($t_{\text{det 1-g}} = 0.11$ s) was three times less than the one in microgravity ($t_{\text{det }\mu\text{-g}} = 0.3$ s). The bubble foot extended much more in μ-g than in 1-g. In Fig. 11, the evolution of the contact angles α and β are also plotted for 1-g. At the beginning, the two contact angles α and β were approximately equal to each other. The bubble was very small and had a symmetrical shape. This suggests that hydrodynamic effects of the flow were not sufficient to overcome the dominancy of the capillary effect. Then, the hydrodynamic effects became more and more important and the symmetry was broken, leading to bubble detachment. The upstream and downstream contact angles increased and decreased, respectively.

From the evolution of the geometrical parameters of the bubbles during their growth, the static and hydrodynamical forces are evaluated. Using a classical point-force approach [51,53,52], a balance on the forces acting on the bubble can be written as:

$$\boldsymbol{F}_B + \boldsymbol{F}_C + \boldsymbol{F}_{CP} + \boldsymbol{F}_D + \boldsymbol{F}_L + \boldsymbol{F}_{AM} = \boldsymbol{0} \tag{6}$$

where $\boldsymbol{F}_B$ is the Archimedean force, $\boldsymbol{F}_C$ the capillary force, $\boldsymbol{F}_{CP}$ the contact pressure force, $\boldsymbol{F}_D$ the drag force, $\boldsymbol{F}_L$ the lift force, and $\boldsymbol{F}_{AM}$ the added mass force. The buoyancy force $\boldsymbol{F}_B$ vanishes under microgravity. The contact pressure force $\boldsymbol{F}_{CP}$ is due to the fact that the bubble is in contact with the wall, instead of being completely surrounded by the liquid, and then to the pressure difference inside and outside the bubble. The pressure difference across the bubble interface at its foot can

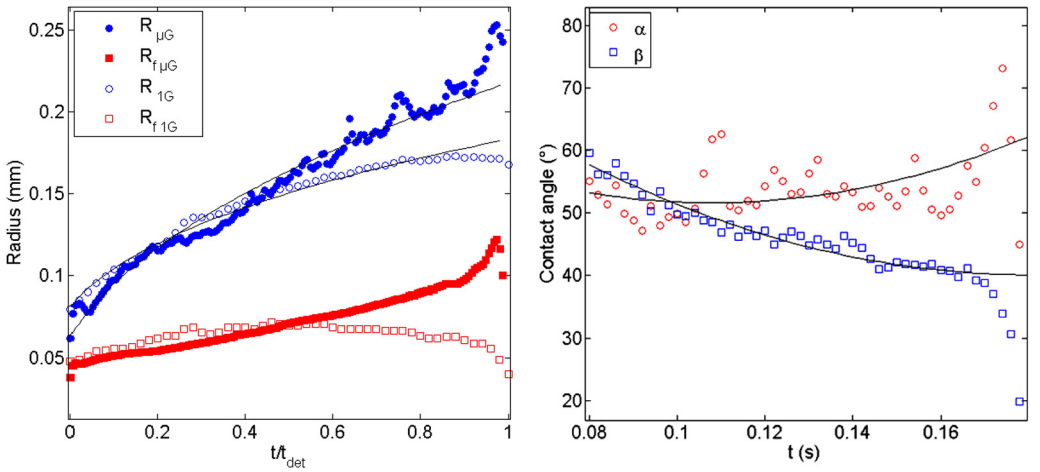

Fig. 11. Evolution of the bubble radius R and bubble foot radius R_f in 1-g and μ-g (left). Evolution of the upstream and downstream contact angles in 1-g.

be expressed versus the equivalent radius at the bubble top R (Laplace equation) and the hydrostatic pressure difference between the bubble top ($y = h$) and the bubble foot ($y = 0$) [60]:

$$\boldsymbol{F}_{\mathrm{CP}} = \left(\frac{2\sigma}{R} + (\rho_{\mathrm{L}} - \rho_{\mathrm{V}})gh\right)\pi R_{\mathrm{f}}^2 \boldsymbol{e}_y \tag{7}$$

The capillary force $\boldsymbol{F}_{\mathrm{C}}$ keeps the bubble foot in contact with the wall. It appears at the triple line (solid–liquid–gas). The expression proposed by Klausner et al. [61] for a circular bubble foot, assuming a linear evolution of the contact angle between α and β, has been extended by Lebon et al. [59] to the case of a non-circular bubble foot, using the approach developed by Dussan et al. [62]. Since the bubble grow was quasi static, the added mass force was negligible in the experiments. The drag force acting in the flow direction and the lift force acting perpendicular to the flow direction can be expressed versus hydrodynamic drag coefficient C_{D} and lift coefficient C_{L}:

$$\boldsymbol{F}_{\mathrm{D}} = \frac{1}{2}\rho_{\mathrm{l}} C_{\mathrm{D}} \pi R^2 (U_{\mathrm{L}} - U_{\mathrm{B}})|U_{\mathrm{L}} - U_{\mathrm{B}}|\boldsymbol{e}_x \quad \text{and} \quad \boldsymbol{F}_{\mathrm{L}} = \frac{1}{2}\rho_{\mathrm{l}} C_{\mathrm{L}} \pi R^2 (U_{\mathrm{L}} - U_{\mathrm{B}})^2 \boldsymbol{e}_y \tag{8}$$

U_{L} and U_{B} being the liquid velocity at the centre of gravity of the bubble and the bubble velocity, respectively.

The expressions for the drag and lift coefficients for a bubble growing on a flow are unknown. Expressions exist for spherical bubbles in the wall vicinity in the limit of small bubble Reynolds number Re_{b} or large bubble Reynolds number. For boiling bubbles, the range of bubble Reynolds numbers is very large, from 1 to 200, in our experiments. Performing several experiments on bubble injection, it was nevertheless possible from Eqs. (6) to (8) and from the expression of the capillary force, to determine an approximated expression for the drag coefficient:

$$C_{\mathrm{D}} = 27 Re_{\mathrm{b}}^{-0.65} \tag{9}$$

Using these expressions for the drag-and-lift coefficient, the different forces acting on a growing bubble in a shear flow in microgravity are plotted in Fig. 12. In the flow direction, the drag force balances the capillary force. In the direction perpendicular to the wall, the contact pressure force balances the capillary force. The lift force is small but not negligible in microgravity.

Additional experiments and direct numerical simulations [63] are still needed to understand the effect of a shear on the bubble hydrodynamics and to be able to predict bubble detachment. The effect of a shear flow on bubble detachment will be also investigated in the RUBI experiment described below thanks to a convection loop, which will create a controlled shear flow above the heater.

3.4. RUBI experiment

In order to evaluate the models quantitatively, generic experiments have to be developed and refined. This is the objective of the RUBI (Reference mUltiscale Boiling Investigation) experiment for the Fluid Science Laboratory on the International Space Station, developed by ESA and several European teams [64,65]. RUBI will provide measurements of wall temperature and heat flux distribution underneath vapour bubbles with high spatial and temporal resolution by means of IR thermography. These data will be synchronised with the bubble shape observation by a high-speed video. Furthermore, the fluid temperature in the vicinity and inside of the bubbles will be measured by an array of four thermocouples. In order to study bubble detachment or sliding on the heating surface, an electrical field can be also applied and a shear flow will be created by a forced convection loop.

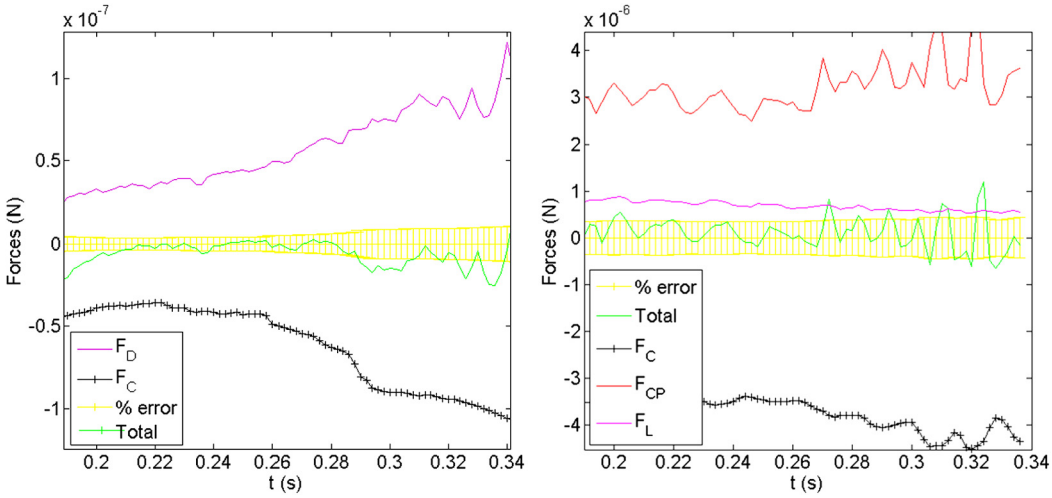

Fig. 12. $U_l = 0.113$ m/s: Force balance parallel to the wall (left) and perpendicular to the wall (right) in μ-g.

In parallel to RUBI, theoretical models for the prediction of heat and mass transfers in the microlayer region at the bubble foot are under development and a benchmark on direct numerical simulation of the bubble growth and detachment would be also interesting to be performed. Then the complementary expertise on experiments, theoretical modelling and numerical simulation should allow making significant progress in the understanding and prediction of the local mechanisms of boiling.

4. Conclusion

Despite the number of experiments on pool boiling in microgravity performed over the past 50 years, the prediction of boiling heat transfer remains a difficult task, which is understandable regarding the numerous involved mechanisms: bubble nucleation, evaporation at the contact line, re-condensation, coalescence, bubble detachment, sliding on the wall. Recent studies have highlighted the role of the heater size, gravity level, subcooling and concentration of dissolved gas on the wall heat flux. At low heat flux, the heat transfer is lower in normal gravity than in microgravity. In normal gravity, bubbles nucleate on the wall and lift-off very quickly. The heated surface is only partially covered by bubbles. In microgravity, even at low heat flux, bubbles nucleate on the wall, coalesce and form a large primary bubble, which has an oscillating motion above the wall. The nucleate boiling regime is fully developed and heat transfer is more efficient than in normal gravity. When the heat flux increases, the tendency is opposite. A partial dry-out of the wall is observed in microgravity and the heat transfer is much less important than in normal gravity. The effect of gravity on heat transfer is well predicted at high wall heat flux. Nevertheless, there is still some work to be done to predict the evolutions observed at low heat flux. Thus correlations are still useful for industrial applications despite their limited range of validity.

From the 2000s, thanks to the development of advanced measurement techniques and the improvement of numerical methods, several analyses were performed at the bubble scale to investigate the local heat and mass transfer around the bubble and at its foot and the bubble detachment mechanisms under an electric field or a shear flow. Several studies have been performed by different teams, mainly in parabolic flights and helped us to design the RUBI experiment for the International Space Station. These objectives should be achieved thanks to complementary approaches based on normal and microgravity experiments, development of theoretical models and direct numerical simulations.

Acknowledgements

The authors would like to thank the “centre national d’études spatiales” (GDR “Microgravité fondamentale et appliquée” and the COMPERE Programme, CT-2540000-1404-CNES-01) and the European Space Agency (MAP Multiscale ANalysis of BOiling Contract 4200020289) for the financial support of their studies, the PhD thesis and post-doc grants, the organisation of the parabolic flights campaigns, and the sounding rocket campaigns.

References

[1] J. Straub, Boiling heat transfer and bubble dynamics in microgravity, Adv. Heat Transf. 35 (2001) 57–172.
[2] H. Ohta, Microgravity heat transfer in flow boiling, Adv. Heat Transf. 37 (2003) 1–76.
[3] P. Di Marco, Review of reduced gravity boiling heat transfer: European research, J. Jpn. Soc. Microgravity Appl. 20 (4) (2003) 252–263.
[4] P. Di Marco, Pool boiling in microgravity: old and recent results, Multiph. Sci. Technol. 19 (2) (2007) 141–165.
[5] J. Kim, Review of nucleate pool boiling bubble heat transfer mechanisms, Int. J. Multiph. Flow 35 (2009) 1067–1076.
[6] H. Merte, J. Clark, Boiling heat transfer with cryogenic fluids at standard, fractional, and near-zero gravity, J. Heat Transf. 86 (1964) 351–359.

[7] R. Siegel, Effects of reduced gravity on heat transfer, Adv. Heat Transf. 4 (1967) 143–228.
[8] M. Zell, J. Straub, A. Weinzierl, Nucleate pool boiling in subcooled liquid under microgravity. Results of texus experimental investigations, in: Proc. 5th European Symposium on Material Sciences under Microgravity, Schloss Elmau, Germany, 1984.
[9] H. Lee, J. Merte, H.F. Chiaramonte, Pool boiling curve in microgravity, J. Thermophys. Heat Transf. 11 (2) (1997) 216–222.
[10] H. Ohta, Experiments on microgravity boiling heat transfer by using transparent heaters, Nucl. Eng. Des. 175 (1997) 167–180.
[11] T. Oka, Y. Abe, Y.H. Mori, A. Nagashima, Pool boiling heat transfer in microgravity (experiments with CFC-113 and water utilizing a drop shaft facility), JSME Int. J. 39 (4) (1996) 798–807.
[12] O. Kannengieser, C. Colin, W. Bergez, Influence of gravity on pool boiling on a flat plate: results of parabolic flights and ground experiments, Exp. Therm. Fluid Sci. 35 (2011) 788–796.
[13] P. Di Marco, W. Grassi, Effect of force fields on pool boiling flow patterns in normal and reduced gravity, Heat Mass Transf. 45 (2009) 959–966.
[14] P. Di Marco, R. Raj, J. Kim, Boiling in variable gravity under the action of an electric field: results of parabolic flight experiments, J. Phys. Conf. Ser. 327 (2011) 012039.
[15] J. Kim, J. Benton, D. Wisniewski, Pool boiling heat transfer on small heaters: effect of gravity and subcooling, Int. J. Heat Mass Transf. 45 (2002) 3919–3932.
[16] D. Christopher, J. Kim, A study of the effects of heater size, subcooling, and gravity level on pool boiling heat transfer, Int. J. Heat Fluid Flow 25 (2004) 262–273.
[17] R. Raj, J. Kim, Heater size and gravity based pool boiling regime map: transition criteria between buoyancy and surface tension dominated boiling, J. Heat Transf. 132 (9) (2010) 091503.
[18] R. Raj, J. Kim, J. Mcquillen, Subcooled pool boiling in variable gravity environments, J. Heat Transf. 131 (9) (2009) 091502.
[19] R. Raj, J. Kim, J. Mcquillen, Gravity scaling parameter for pool boiling heat transfer, J. Heat Transf. 132 (9) (2010) 091502.
[20] R. Raj, J. Kim, J. Mcquillen, On the scaling of pool boiling heat flux with gravity and heater size, J. Heat Transf. 134 (2012) 011502.
[21] V.K. Dhir, G.R. Warrier, E. Aktinol, D. Chao, J. Eggers, W. Sheredy, W. Booth, Nucleate pool boiling experiments (NPBX) on the international space station, Microgravity Sci. Technol. 24 (5) (2012) 307–325.
[22] R. Raj, J. Kim, J. Mcquillen, Pool boiling heat transfer on the international space station: experimental results and model verification, J. Heat Transf. 134 (2012) 101504.
[23] J.F. Zhao, J. Li, N. Yan, S.F. Wang, Bubble behavior and heat transfer in quasi steady pool boiling in microgravity, Microgravity Sci. Technol. 21 (2009) 175–183.
[24] G.R. Warrier, V.D. Dhir, D.F. Chao, Nucleate Pool Boiling eXperiment (NPBX) in microgravity: international space station, Int. J. Heat Mass Transf. 83 (2015) 781–798.
[25] O. Kannengieser, C. Colin, W. Bergez, Pool boiling with non-condensable gas in microgravity: results of a sounding rocket experiment, Microgravity Sci. Technol. 22 (2010) 447–454.
[26] M. Sagan, Simulation numérique directe et étude expérimentale de l'ébullition nucléée en microgravité: application aux réservoirs des moteurs d'Ariane, PhD thesis, University of Toulouse, France, 2013, http://ethesis.inp-toulouse.fr/archive/00002609/.
[27] J. Kim, R. Raj, Gravity and Heater Size Effects on Pool Boiling Heat Transfer, Report NASA/CR-2014-216672.
[28] P. Di Marco, W. Grassi, Pool boiling in reduced gravity, Multiph. Sci. Technol. 13 (3) (2001) 179–206.
[29] W.M. Rohsenow, A method of correlating of heat transfer data for surface boiling of liquids, Trans. Am. Soc. Mech. Eng. 84 (1952) 969–975.
[30] K. Stephan, M. Abdelsalam, Heat-transfer correlation for natural convection boiling, Int. J. Heat Mass Transf. 23 (1980) 73–87.
[31] M. Cooper, Correlation for nucleate boiling – formulation using reduced pressure, Physicochem. Hydrodyn. 3 (1982) 89–111.
[32] V.K. Dhir, Nucleate boiling, in: S. Kandlikar, M. Shoji, V.K. Dhir (Eds.), Handbook of Phase Change – Boiling and Condensation, vol. 4.4, Taylor and Francis, 1999, pp. 86–89.
[33] O. Kannengieser, Étude de l'ébullition sur plaque plane en microgravité, application aux réservoirs cryogéniques des fusées Ariane V, PhD thesis, INP Toulouse, 2009, http://ethesis.inp-toulouse.fr/archive/00001058/.
[34] D. Qui, V. Dhir, Single-bubble dynamics during pool boiling under low gravity conditions, J. Thermophys. Heat Transf. 16 (3) (2002) 336–345.
[35] D.M. Qui, V.K. Dhir, D. Chao, M.M. Hasan, E. Neumann, G. Yee, A. Birchenough, Single bubble dynamics during pool boiling under low gravity conditions, J. Thermophys. Heat Transf. 16 (2002) 336–345.
[36] C. Sodtke, J. Kern, N. Schweizer, P. Stephan, High-resolution measurements of wall temperature distribution underneath a single vapour bubble under microgravity conditions, Int. J. Heat Mass Transf. 49 (2006) 1100–1106.
[37] N. Schweizer, P. Stephan, Experimental study of bubble behavior and local heat flux in pool boiling under variable gravitational conditions, J. Multiph. Sci. Technol. 21 (4) (2009) 329–350.
[38] E. Wagner, C. Sodtke, N. Schweizer, P. Stephan, Experimental study of nucleate boiling heat transfer under low gravity conditions using TLCs for high resolution temperature measurements, J. Heat Mass Transf. 42 (10) (2006) 875–883.
[39] E. Wagner, P. Stephan, High resolution measurements at nucleate boiling of pure FC-84 and FC-3284 and it binary mixtures, J. Heat Transf. 131 (12) (2009) 121008.
[40] P.C. Stephan, C.A. Busse, Analysis of the heat transfer coefficient of grooved heat pipe evaporator walls, Int. J. Heat Mass Transf. 35 (1992) 383–391.
[41] V. Nikolayev, Dynamics of the triple contact line on a nonisothermal heater at partial wetting, Phys. Fluids 22 (2010) 082105.
[42] A. Rednikov, P. Colinet, Evaporation-driven contact angles in a pure-vapor atmosphere: the effect of vapor pressure non-uniformity, Math. Model. Nat. Phenom. 7 (4) (2012) 53–63.
[43] G. Son, V.K. Dhir, N. Ramanujapu, Dynamics and heat transfer associated with a single bubble during nucleate boiling on a horizontal surface, J. Heat Transf. 121 (1999) 623–631.
[44] T. Fuchs, J. Kern, P. Stephan, A transient nucleate boiling model including microscale effects and wall heat transfer, in: Special Issue on Boiling, Two-Phase Flow Heat Transfer and Interfacial Phenomena, J. Heat Transf. 128 (12) (2006) 1257–1265.
[45] C. Kunkelmann, P. Stephan, CFD simulation of boiling flows using the volume-of-fluid method within OpenFOAM, J. Numer. Heat Transf., Part A, Appl. 56 (8) (2009) 631–646.
[46] C. Kunkelmann, P. Stephan, Numerical simulation of the transient heat transfer during nucleate boiling of refrigerant HFE-7100, Int. J. Refrig. 33 (2010) 1221–1228.
[47] P. Di Marco, Bubble growth and detachment: current status and future prospects, in: Proc. HEAT 2008, Fifth International Conference on Transport Phenomena in Multiphase Systems, Bialystok, Poland, 30 June–3 July 2008, pp. 67–82 (invited paper).
[48] A. Cattide, P. Di Marco, W. Grassi, Evaluation of the electrical forces acting on a detaching bubble, in: Proc. XXV UIT National Conference, Trieste, Italy, 2007, pp. 315–320.
[49] P. Di Marco, R. Kurimoto, G. Saccone, K. Hayashi, A. Tomiyama, Bubble shape under the action of electric forces, Exp. Therm. Fluid Sci. 49 (2013) 160–168.
[50] P. Di Marco, Influence of force fields and flow patterns on boiling heat transfer performance, keynote lecture, in: Proc. of the International Heat Transfer Conference, IHTC14, Washington, DC, USA, 2010, IHTC14-23409, 18 pp. (CD-ROM).
[51] G.E. Thorncroft, J.F. Klausner, R. Mei, Bubble forces and detachment models, Multiph. Sci. Technol. 13 (2001) 35–76.

[52] C.W.M. Van Der Geld, The dynamics of a boiling bubble before and after detachment, Heat Mass Transf. 45 (2009) 831–846.
[53] G. Duhar, G. Riboux, C. Colin, Vapour bubble growth and detachment at the wall of shear flow, Heat Mass Transf. 45 (2009) 847–855.
[54] D. Legendre, C. Colin, T. Coquard, Hydrodynamic of a hemispherical bubble sliding and growing on a wall in a viscous linear shear flow, Philos. Trans. R. Soc. A 366 (2008) 2233–2248.
[55] Y. Ma, J.N. Chung, A study of bubble dynamics in reduced gravity forced-convection boiling, Int. J. Heat Mass Transf. 44 (2001) 399–415.
[56] D. Serret, D. Brutin, O. Rahli, Convective boiling between 2D plates: microgravity influence on bubble growth and detachment, Microgravity Sci. Technol. 22 (3) (2010) 377–384.
[57] H. Yoshikawa, C. Colin, Single vapor bubble behavior in a shear flow in microgravity, in: 7th International Conference on Multiphase Flows, Tampa, FL, USA, June 2010.
[58] C.W.M. Van Der Geld, C. Colin, Q.I.E. Segers, Da Rosa V.H. Pereira, H.N. Yoshikawa, Forces on a boiling bubble in a developing boundary layer, in microgravity with g-jitter and in terrestrial conditions, Phys. Fluids 24 (2012) 082104, http://dx.doi.org/10.1063/1.4743026.
[59] M. Lebon, H. Yoshikawa, J. Sebilleau, C. Colin, Bubble formation in a quiescent liquid and in a shear flow, in: 9th International Conference on Boiling and Condensation Heat Transfer, Boulder, CO, USA, 26–30 April 2015.
[60] G. Duhar, C. Colin, Dynamics of Bubble growth and detachment in a viscous shear flow, Phys. Fluids 18 (2006) 077101.
[61] J.F. Klausner, R. Mei, M.D. Bernhard, L.Z. Zeng, Vapor bubble detachment in forced convection boiling, Int. J. Heat Mass Transf. 36 (1993) 651–662.
[62] E.B. Dussan, R. Tao-Ping, Chow, On the ability of drops or bubbles to stick to non-horizontal surfaces of solids, J. Fluid Mech. 137 (1983) 1–29.
[63] D. Li, V.K. Dhir, Numerical study of single bubble dynamics during flow boiling, J. Heat Transf. 129 (2007) 864–876.
[64] N. Schweizer, M. Stelzer, O. Schoele-Schulz, G. Picker, H. Ranebo, J. Dettmann, O. Minster, B. Toth, J. Winter, L. Tadrist, P. Stephan, W. Grassi, P. Di Marco, C. Colin, G.P. Celata, J. Thome, O. Kabov, RUBI—a reference multiscale boiling investigation for the fluid science laboratory, in: 38th COSPAR Scientific Assembly, Bremen, Germany, 18–15 July 2010, p. 18, http://adsabs.harvard.edu/abs/2010cosp...38.3565S.
[65] B. Toth, et al. Future ESA experiments in heat and mass transfer research on-board the international space station, in: Proc. Seventh International Symposium on Two-Phase Systems for Ground and Space Applications, Beijing, China, 17–21 September 2012.